DOI: 10.61782/fa.2025.0038

FORUM ACUSTICUM
EURONOISE 2025

A STATISTICAL REGRESSION FRAMEWORK FOR EVALUATING NOISE EXPOSURE THROUGH OUTDOOR-TO-INDOOR SOUND PROPAGATION MODELS

Michail Evangelos Terzakis* **Cédric Van hoorickx** **Maarten Hornikx**

Building Acoustics Group, Department of the Built Environment,
Eindhoven University of Technology, Eindhoven, The Netherlands

ABSTRACT

Urban noise exposure has been shown to have significant adverse effects on human health. Studies based on outdoor noise levels, rather than indoor levels, risk introducing bias when identifying an exposure-response relationship with health outcomes. This bias is of particular concern for vulnerable groups (e.g., children) who spend most of their time indoors. This highlights the need for a comprehensive approach to modelling outdoor-to-indoor sound propagation for the estimation of indoor noise levels. For both outdoor and indoor propagation, energetic approaches are used, while the facade sound insulation is modeled via the Transfer Matrix Method, incorporating the facade element size and bridge connections. Validation of this modelling approach against sound insulation measurements has revealed good agreement. The employment of the developed models resulted in the generation of datasets, facilitating the implementation of statistical learning (random forest) models for estimating (equivalent) indoor noise levels using predictors associated with outdoor levels and factors related to the indoor and outdoor environment, and facade structure. The proposed approach has the potential to estimate indoor levels for entire cities from predicted outdoor noise levels (noise maps) and built environment characteristics.

Keywords: *outdoor-to-indoor, sound propagation, sound insulation, modelling.*

***Corresponding author**: *m.e.terzakis@tue.nl.*

1. INTRODUCTION

Urban noise exposure has been characterized as a threat for people, showing significant associations with psychophysiological, mental health, cognitive, and sleep aspects [1, 2]. Noise exposure studies are usually conducted via the outdoor noise levels rather than the indoor levels [2]. This may correspond to a systematic risk of bias in the identification of "true" exposure-response relationship with health outcomes [3]. This bias is of particular concern for vulnerable groups (e.g. children) who spend the majority of their time indoors.

To properly characterize the indoor noise exposure, various approaches have been defined to simulate the sound propagation from outdoors to indoors via building façade structures (e.g. [3–6]). In noise exposure studies, the utilisation of the auralisation-based approaches (e.g., [5, 6]) can be regarded as a strategy for characterizing the outdoor-to-indoor sound propagation in a detailed way. For adjacent room settings subjected to diffuse-field conditions, auralization approaches for airborne sound insulation based on ISO 12354-1 [7] were proposed [8, 9]. Based on these approaches, auralization models for both adjacent indoor and outdoor-indoor settings were proposed [5], using closed form formulae for sound insulation. For outdoor and indoor settings, an alternative approach was proposed, where the sound insulation was modeled via closed form formulae and a spatial window technique (size correction) [10]. However, the aforementioned approaches were based on single-layer and -component structures.

The objective of this study is to develop a modelling approach for the propagation of sound from outdoors to indoors via multi-layer and multi-component façade structures and apply this approach through generated datasets for evaluating noise exposure via a statistical regression framework. This approach facilitates the simulation of a broad range of built environments, enabling the estimation of indoor noise exposure levels based on, for instance, noise maps of the outdoor noise exposure level as well as the evaluation of the significance of diverse predictors.

2. MODELING FORMULATION

2.1 Façade Sound Insulation Modelling

Although numerical modelling approaches, such as the Finite Element Method (FEM) [11] and the Boundary Element Method (BEM) [12], can be applied for the computation of sound insulation in a precise way, these modelling approaches require high computational complexity. Alternatively, the Transfer Matrix Method (TMM) can provide a formulation for the calculation of the sound insulation of structures in an efficient way, considering the propagation of sound waves through multi-layered structures [13].

2.1.1 Infinite Incident Sound Transmission Coefficient

In the TMM framework [13], a plane wave impinges on the first layer of a material under an angle of incidence θ (i.e. angle between the direction of propagation of the incident plane wave and the normal to the plane of the layer) and propagates into the cavity, and then to a second material layer, and so on, up to the radiation (last) layer.

Assuming a multi-layer structure subject to thin-plate theory, a simple product among the transfer matrices of thin plates and fluid cavities, including the incident and radiated layer, results in the infinite sound transmission coefficient [13, 14]. However, in structures composed of diverse media (e.g. solid and poroelastic), the aforementioned conventional approach is untenable. Coupling interface matrices are included to global matrix, composed of the transfer matrices of the diverse layers, to satisfy the continuity condition between two adjacent elements and for calculating the infinite sound transmission coefficient [13].

2.1.2 Spatial Windowing Technique

A spatial windowing technique has been introduced to alleviate infinite structure behaviour effects at low frequencies via the radiation efficiency of finite size structure [10]. Considering rectangular surfaces, an efficient methodology for calculating the radiation efficiency was proposed in [15]. Based on this approach, the adjusted radiation efficiency was proposed in [16] for calculating the radiation efficiency of rectilinear surfaces (polygon surfaces in which all sides intersect at right angles) by dividing the rectilinear surfaces into isolated and adjacent (first order correlation) sub-domains (sub-surfaces).

2.1.3 Finite Incident Sound Transmission Coefficient

For calculating the sound transmission coefficient ($\tau_{\text{fin}}(\theta)$) for rectangular surfaces, the spatial windowing technique can be implied to the (infinite) incident sound transmission coefficient. Regarding a single-layer structure, the finite sound transmission coefficient can be obtained as in [17], while for a multi-layer structures, the finite sound transmission coefficient can be obtained as in [10]. For rectilinear surfaces, the same approaches can be applied so that the finite (first-order) sound transmission coefficient to be obtained as in [16].

2.1.4 Bridge Connection

The bridge connection (line or point) can be further incorporated into the finite incident sound transmission coefficient, providing a correction at high frequencies. In double-layer structures, the studs can be incorporated using a thin-plate [18] and a global matrix [19] approach.

2.2 Propagation Modelling

An example room with total dimensions 3m×3m×3m (L×W×H) was considered, assuming that its façade structure consists of a single-layer rectilinear wall (concrete of thickness 0.1m) and a single-layer (1m×1m) rectangular window (glass of thickness 0.006m) component, both of which subject to the thin-plate theory. Their material properties were taken from [16]. Furthermore, 11 sound sources (S1–S11) located in front of the façade structure were considered (road-traffic structure), covering a total length of 14m. These sound sources were positioned at three different distances from the façade (7m, 14m, and 21m), denoting the sound source formats (L1–L3). Finally, five receivers are included indoors. R1: at the centre of the room; R2: at 0.5m from the front and left wall; R3: at 0.6m from the front and right wall; R4 at 0.7m from the back and left wall; R5 at 0.4m from the back and right wall. The height of all receivers was kept constant at 1m from the ground (children's ear seated). An illustration is presented in Fig. 1.

2.2.1 Outdoor-to-Façade Propagation Modelling

For point sources with acoustic power 1W, the free-field mean squared sound pressure at any point of the iso-

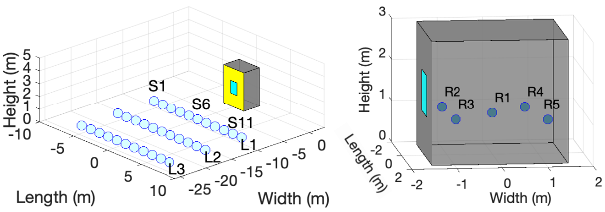

Figure 1. Representation of the example scenario.

lated and adjacent surfaces ss at a distance r_{s} from the sound source s can be expressed as $p_{\mathrm{ss}}^2(f, r_{\mathrm{s}}) = Z_0(\frac{1}{4\pi r_{\mathrm{s}}^2})$. Hence, the incident sound power at any point of façade under free-field conditions can be expressed as [5]

$$W_{\mathrm{inc,s}}(f, \theta_{\mathrm{s}}, r_{\mathrm{s}}) = \frac{1}{4\pi} \int_{S_{\mathrm{ss}}} \frac{1}{4\pi r_{\mathrm{s}}^2} |\cos(\theta_{\mathrm{s}})| \mathrm{d}S. \tag{1}$$

For small elements and source positions that are far away, a first-order approximation can be made by assuming that θ_{s} and r_{s} do not vary significantly in S_{ss}.

2.2.2 *Façade-to-Indoor Propagation Modelling*

In façade-to-indoor propagation modelling, it was assumed that the façade elements act as sound sources. By further assuming that each sub-surface emits sound into a hemisphere, the squared pressure from the wall (p_{w}^2) and window (p_{g}^2) surface to the receiver q in the room R can be calculated as [5]

$$p_{\mathrm{w},q}^2(f) = Z_0 \Bigg[\sum_i \sum_{\substack{j \in \epsilon_i \\ j > i}} W_{\mathrm{tr},ij,\mathrm{w}}(\theta_{s,ij}) \left(\frac{2}{4\pi r_{ij,q}^2} + \frac{4}{A_{\mathrm{R}}(f)} \right) - \sum_i \sum_i W_{\mathrm{tr},i,\mathrm{w}}(\theta_{s,i}) \left(\frac{2}{4\pi r_{i,q}^2} + \frac{4}{A_{\mathrm{R}}(f)} \right) \Bigg] \tag{2}$$

$$p_{\mathrm{g},q}^2(f) = Z_0 \left[W_{\mathrm{tr},i,\mathrm{g}}(\theta_{\mathrm{s},i}, r_{\mathrm{s}}) \left(\frac{2}{4\pi r_{i,q}^2} + \frac{4}{A_{\mathrm{R}}(f)} \right) \right], \tag{3}$$

where the transmitted sound power is defined as $W_{\mathrm{tr}} = W_{\mathrm{inc,s}} \cdot \tau_{\mathrm{fin}}$. Note that the τ_{fin} term is defined in Section 2.1.3. Furthermore, $r_{ij,q}$ and $r_{i,q}$ denote the distance between the center of adjacent and isolated sub-domains and receiver q, respectively, and A_{R} denotes the total absorption area of the room.

2.3 Outdoor-based Indoor Impulse Response

The outdoor-based indoor impulse response per sound source and indoor receiver position can be synthesized via the inverse Fourier Transform of the sum of the frequency responses of the wall ($H_{\mathrm{w},q}$) and window ($H_{\mathrm{g},q}$) surfaces expressed as $h_q(t) = \mathfrak{F}^{-1}\{H_{\mathrm{w},q}(f) + H_{\mathrm{g},q}(f)\}$. The latter frequency responses can be calculated using the approach outlined in [5].

Finally, since the sound transmission coefficient is calculated for 31 1/3-octave frequency bands, ranging from 20Hz to 20kHz, a linear interpolation and a piecewise cubic extrapolation in the sound transmission coefficient is employed within the frequency range from zero to Nyquist frequency. Additionally, a linear (antisymmetric) phase term based on [20] is added to $H_{\mathrm{w},q}$ and $H_{\mathrm{g},q}$ for synthesizing the outdoor-based indoor impulse response, expressed as [5, 6] $\tau_{\mathrm{fin}}(\theta) = |\tau_{\mathrm{fin}}(\theta)| e^{j\phi(f)}$.

3. RESULTS AND DISCUSSION

3.1 Modelling Example

Based on the example described in Section 2.2, the finite sound reduction index of the window and wall surfaces is calculated via the methodologies presented in Section 2.1. The results are presented in Fig. 2.

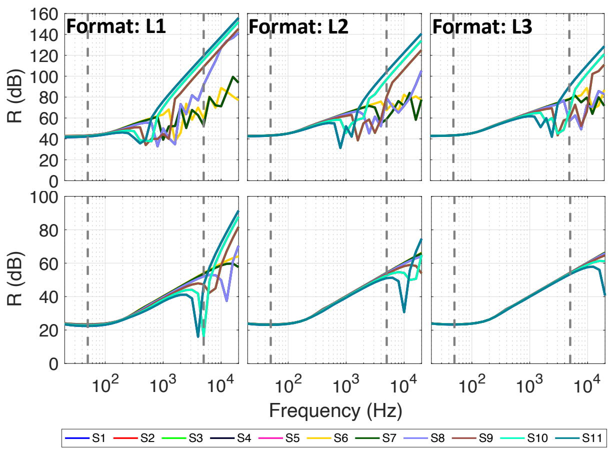

Figure 2. Sound reduction index of the wall (top) and glass (bottom) surface per source and format.

Focusing on Fig. 2 (top), the influence of all adjacent and isolated sub-surfaces to the sound reduction index of the wall surface is illustrated, similar to those presented in [16]. Since the sound source positions S1-S5 are symmetrical to those of S7-S11, the sound reduction indexes of the former are obscured by the latter. For the window surface Fig. 2 (bottom), analogous sound reduction trends to those exhibited by the wall surface are evident.

By incorporating the outdoor and indoor modelling, the outdoor-based indoor impulse and frequency responses can be synthesized with respect to five receiver positions. The results are illustrated in Fig. 3.

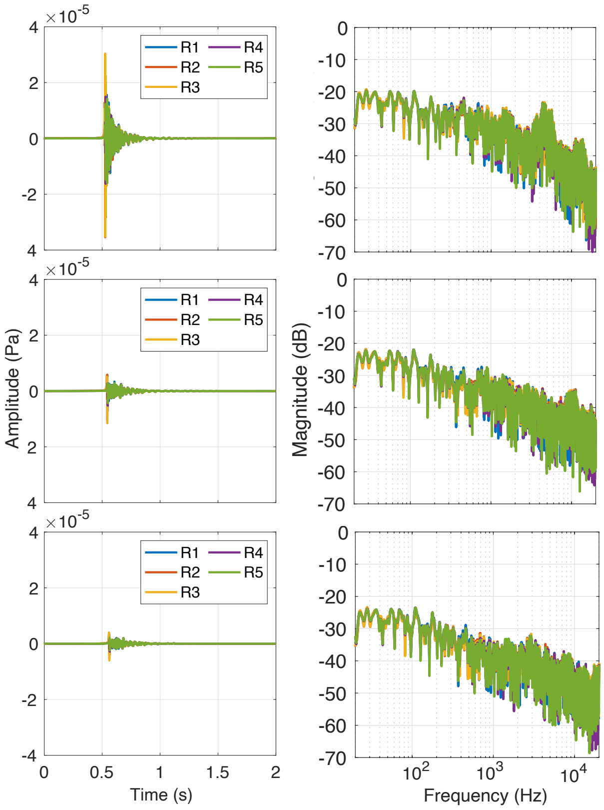

Figure 3. Average impulse and magnitude responses per receiver position across the sound sources (S1-S11) in Format L1 (top), L2 (mid), and L3 (bottom).

Regarding Fig. 3, the presence of multiple peaks in the magnitude responses denotes the (average) sound transmission from the elements of the façade structure. The most prominent peaks are presented in relation to the Format L1 among the three formats. As the distance between the sound source format and façade structure increases (from Format L1 to Format L3), a single incident character is obtained. Finally, the impact of the wall surface is only evident in the coincidence region, while in other regions, the glass surface dominates the wall surface in the total sound reduction index [16].

3.2 Experimental Validation

For validating the modeling methodology, the settings and the results of the case study presented in [21] for a 201.6m^3 lecture room were used with respect to the distribution of sound sources in the linear format. Regarding the characteristics of façade structure from inside to outside, this consists of a plaster layer, a brick layer, a poroelastic layer (mineral wool) and a steel layer with point connections. For simplicity, it was assumed that the façade structure consists of a three-layer structure composed by a brick layer ($\rho = 1900$ kg/m^3, $E = 2.4 \cdot 10^{10}$ Pa, $\mu = 0.1$, $\eta = 0.01$, and $h = 0.050$ m), a poroelastic layer ($\phi = 0.9$, $\alpha_\infty = 1$, $\sigma = 59100$ NS/m^4, $\Lambda = 10\mu$ Pa, $\Lambda' = 36\mu$ Pa, $\rho = 90$ kg/m^3, $E = 7 \cdot 10^5$ Pa, $\mu = 0.01$, $\eta = 0.01$, and $h = 0.070$ m), and a steel layer ($\rho = 7800$ kg/m^3, $E = 2.1 \cdot 10^{11}$ Pa, $\mu = 0.33$, $\eta = 0.01$, and $h = 0.026$ m), assuming that the plaster layer does not significantly influence the sound reduction index. Regarding windows, these consist of a double-leaf structure, where the thickness of each layer is 5mm and the gap between the two panes is 15mm. The reverberation time of the room was obtained via ISO 3382-2 [22]. The comparison between measured and predicted sound insulation is presented in Fig. 4.

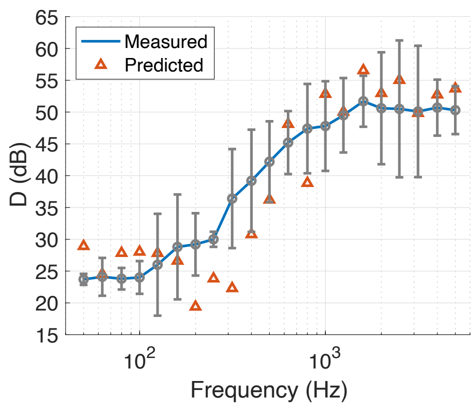

Figure 4. Comparison between the measured and calculated sound insulation, expressed via the level difference (D) in 1/3-octave frequency bands. The error-bars represent the 95% Confidence Interval.

In Fig. 4, the predicted and measured results present a good agreement. The observed discrepancies can be attributed to various factors, including deviations in the material properties, the incident field, the modal behaviour of surfaces and room, and the effect of window frames.

3.3 Application

Based on the developed modelling methodology, datasets can be generated for developing statistical learning prediction models for estimating the indoor noise exposure levels, expressed by the equivalent noise indicators, via various predictors. These predictors correspond to the outdoor noise exposure levels and factors related to outdoor environment, indoor environment, and façade structures. This approach allows for estimating the indoor noise exposure levels in areas with available outdoor levels and built environment characteristics. The block-diagram of application is presented in Fig. 5.

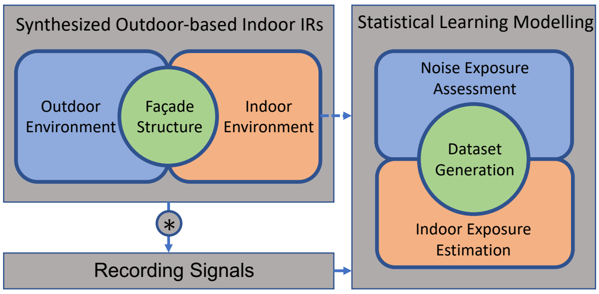

Figure 5. Application of outdoor-to-indoor models. Note that the dashed arrow denotes the additional parameters related to the outdoor and indoor environment as well as façade structure.

3.3.1 *Dataset Generation*

First, the impact of the room size was considered, defining three rooms (L×W×H): Room 1 (3×3×3), Room 2 (4×4×3), and Room 3 (5×4×4). Second, the façade structures were considered, defining two types of wall structures (i.e., monolithic, and filled-cavity) subject to the global-matrix approach, and three types of windows (i.e., single-leaf, double-leaf, and triple-leaf) subject to the thin-plate approach. In both wall structures, each (solid) leaf has a thickness of 0.1m and 0.2m. In the filled-cavity wall structures, a mineral wool material was considered for the cavity measuring 0.1m, while point connections ($n = 10$) between the leaves were also taken into account. Regarding the window panes, the thickness of the leafs and the (air fluid) cavity depths were set to 4mm, 8mm, and 12mm. The dimensions of the windows per room scenario are presented in Tab. 1. Finally, four façade structures composed of wall and window structures were considered: (a) single-leaf wall with single-leaf window, (b) double-leaf wall with single-leaf window, (c) double-leaf wall with double-leaf window, and (d) double-leaf wall with triple-leaf window. It should be noted that the generated dataset is constrained to the information deemed necessary for a city.

Table 1. Window scenarios (WSc) per room (R).

R	WSc	L_g(m)	H_g(m)	R	WSc	L_g(m)	H_g(m)
R1	W1.1	0.50	0.50	R3	W3.1	0.50	0.50
	W1.2	1.00	1.00		W3.2	1.00	1.00
	W1.3	2.00	2.00		W3.3	2.00	2.00
R2	W2.1	0.50	0.50		W3.4	2.50	2.50
	W2.2	1.00	1.00		W3.5	3.00	3.00
	W2.3	2.00	2.00		W3.6	3.50	3.50
	W2.4	2.50	2.50				

3.3.2 *Noise Exposure Assessment*

By convolving the synthesized outdoor-based indoor impulse responses with road-traffic (1-minute) recordings, the noise exposure indoors can be estimated. Similarly, the outdoor noise exposure levels can be estimated at the center of the façade structures. For the assessment of the relationship between indoor and outdoor noise exposure, the equivalent noise indicator can be calculated for one second integration time. The assessed relationships with respect to R1, Format L1 (defined in Fig. 1), and window size W1.2 per façade structure (defined in Section 3.3.1) are presented in Fig. 6.

As illustrated in Fig. 6 (top), the improvement of façade configuration with respect to the window surface leads to a reduction in equivalent indoor noise exposure levels. A lack of a significant effect of two wall thicknesses is also evident, as confirmed by the averaged spectral outdoor-to-indoor level difference presented in Fig. 6 (bottom). Although not shown here, as the surface area of window increases, the effect of wall structure is reduced, while the effect of window becomes dominant. The coincidence frequency of the thinner single wall surface is approximately 500Hz, while for the thicker single wall structure, the coincidence frequency is lower, at around 250Hz. Furthermore, it can be observed that their mass-air-mass and mass-air-mass-air-mass resonance frequencies exhibit a concurrence with the lowest coincidence frequencies of the wall surface.

3.3.3 *Prediction Modelling and Verification*

In order to estimate the equivalent indoor noise exposure levels ($L_{\mathrm{eq,In}}$), averaged over a fifteen-second period, the random forest (RF) modelling approach [23] was

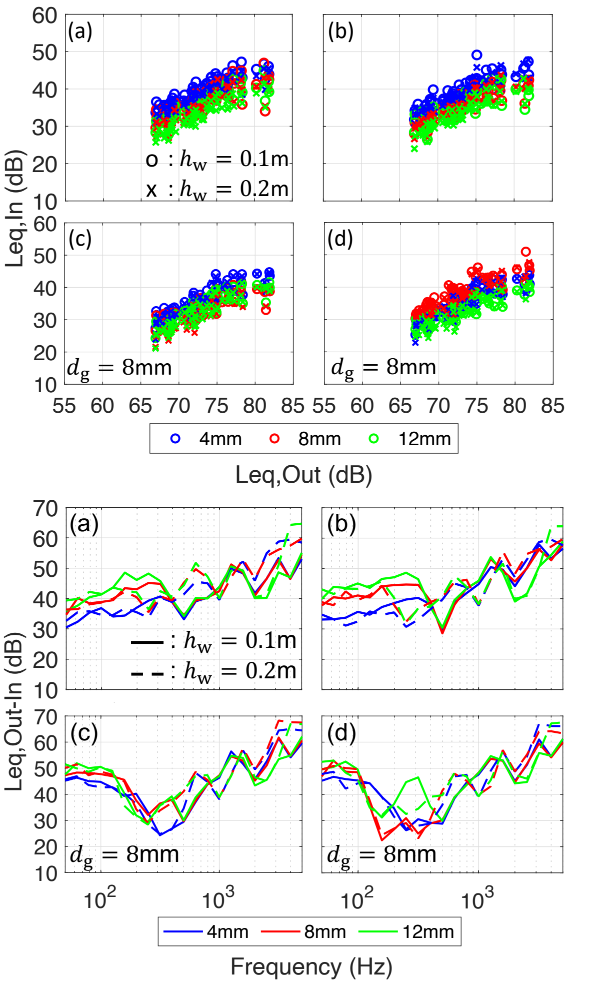

Figure 6. Relationship between the average outdoor and indoor levels (top) and time-averaged equivalent spectral outdoor-to-indoor level differences (bottom) with respect to Format L1, R1, and W1.2 per façade structure (a-d). Note that h_w denotes the thickness of the wall, while d_g denotes the window cavity width.

employed in the generated dataset via the *ranger* package [24] in RStudio. The outdoor noise exposure levels ($L_{\mathrm{eq,Out}}$) at the centre of the façade are considered, in conjunction with parameters associated with the outdoor environment (FrmtDist: format distance), the indoor environment (RoomVol: room volume), and façade structure (SRatio: window-façade ratio, hGlass: glass thickness, hWall: wall thickness, dGlass: distance between glass panes, WinStruct: window structure, and WinStruct: wall structure). Note that the WinStruct and WallStruct predictors are categorical predictors while all the others are continuous predictors. The dataset, composed by 28080 observations (sound levels) were split into a 70% for training and a 30% for testing. For tuning of the RF models, the number of trees (n_{tr}) was selected to range from 100 to 1200 trees with an increment of 100 trees, while the number of split-variables (m_{tr}) was set to vary from 3 to 9 variables with an increment of 1 variable. The node size was ranged from 1 node to 15 nodes with an increment of 1 node. Following the tuning procedure, $n_{\mathrm{tr}} = 900$, $m_{\mathrm{tr}} = 5$, predictors $= 9$, and node size $= 4$.

For exploring the impact of the various predictors, the (normalized) importance of each predictor in the model was assessed, and the results are presented in Fig. 7.

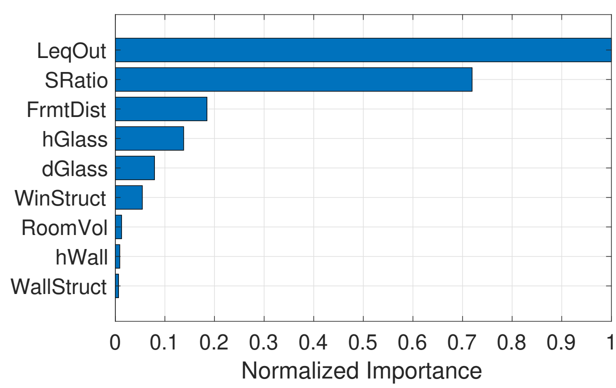

Figure 7. Importance of predictors.

As seen from Fig. 7, the outdoor noise exposure levels and the ratio between the window and façade surface correspond to the most important predictors, indicating that these predictors explained the highest percentage of the unexplained variance in the model. The wall parameters presented the less significant contribution to the model, which is also validated from Fig. 6.

Finally, the k-fold cross-validation procedure for $k = 10$ was adopted [25], splitting the training dataset into ten equal in-size chunks and adopting a resampling procedure. The model was developed based on nine chunks, with the objective of predicting the tenth treated as a validation set. The performance of the fitting model was evaluated via the R^2 and RMSE metric [26]. The results are presented in Fig. 8.

As seen from Fig. 8, the RF modelling approach presented a RMSE $= 1.67$dB with respect to the test dataset. By interpreting the error level with the ability of a healthy ear to perceive a change in broadband noise levels, cor-

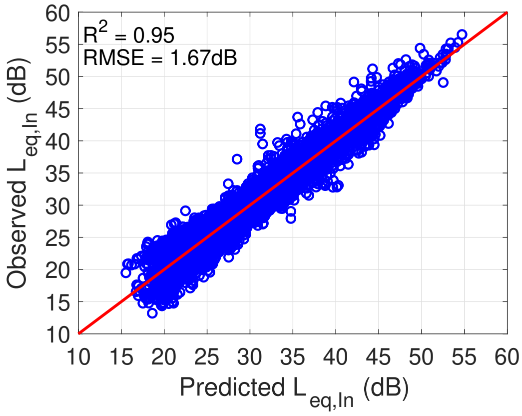

Figure 8. Modelling validation.

responding to the perceptible level difference [27]. An error level around 3dB is associated to a just audible level difference, indicating a good performance of the executed modeling approach, as the RMSE level falls below this threshold.

4. CONCLUSIONS

In this paper, an outdoor-to-indoor modelling framework, validated via sound insulation measurements, was developed. The objective of this approach is to support noise exposure studies via generated (modelling-based) datasets so that the indoor noise exposure levels can be estimated via statistical learning approaches. This approach enables a detailed and controlled characterisation of outdoor-to-indoor sound propagation, which has the potential to estimate indoor levels in cities with available predicted outdoor noise levels and built environment characteristics.

5. ACKNOWLEDGMENTS

This research was funded by the European Union's Horizon 2020 research and innovation program under grant agreement No. 874724, Equal-Life Project, part of the European Human Exposome network.

6. REFERENCES

[1] I. van Kamp, S. Simon, H. Notley, C. Baliatsas, and E. van Kempen, "Evidence Relating to Environmental Noise Exposure and Annoyance, Sleep Disturbance, Cardio-Vascular and Metabolic Health Outcomes in the Context of IGCB (N): A Scoping Review of New Evidence," *International Journal of Environmental Research and Public Health*, vol. 17, p. 3016, 4 2020.

[2] M. E. Terzakis, M. Dohmen, I. van Kamp, and M. Hornikx, "Noise Indicators Relating to Non-Auditory Health Effects in Children—A Systematic Literature Review," *International Journal of Environmental Research and Public Health*, vol. 19, p. 15633, 11 2022.

[3] M. Terzakis, C. Van hoorickx, M. Hornikx, F. Naim, A. Hansell, and J. Gulliver, "Estimation of Low Frequency Outdoor-to-indoor Noise Attenuation Factors Based on Night-time Noise Exposure," in *30th International Congress on Sound and Vibration (ICSV)*, (Amsterdam, The Netherlands), pp. 1–8, 2024.

[4] B. Locher, A. Piquerez, M. Habermacher, M. Ragettli, M. Röösli, M. Brink, C. Cajochen, D. Vienneau, M. Foraster, U. Müller, and J. Wunderli, "Differences between Outdoor and Indoor Sound Levels for Open, Tilted, and Closed Windows," *International Journal of Environmental Research and Public Health*, vol. 15, 1 2018.

[5] I. Muhammad, A. Heimes, and M. Vorländer, "Interactive real-time auralization of airborne sound insulation in buildings," *Acta Acustica*, vol. 5, p. 19, 4 2021.

[6] I. Muhammad, A. Heimes, and M. Vorländer, "Sound insulation auralization filters design for outdoor moving sources," in *PROCEEDINGS of the 23rd International Congress on Acoustics*, (Aachen, Germany), pp. 1721–1728, 2019.

[7] ISO, "ISO 12354-1 Building acoustics Estimation of acoustic performance of buildings from the performance of elements Part 1: Airborne sound insulation between rooms," *International Organization for Standardization*, 2017.

[8] M. Vorländer and R. Thaden, "Auralisation of airborne sound insulation in buildings," *Acta Acustica*, vol. 86, pp. 70–76, 2000.

[9] A. Rodríguez-Molares, "A new method for auralisation of airborne sound insulation," *Applied Acoustics*, vol. 74, pp. 116–121, 1 2013.

[10] M. Villot, C. Guigou, and L. Gagliardini, "Predicting the Acoustical Radiation of Finite Size Multi-layered Structures by Applying Spatial Windowing on Infinite Structures," *Journal of Sound and Vibration*, vol. 245, pp. 433–455, 8 2001.

[11] N. Atalla and F. Sgard, *Finite element and boundary methods in structural acoustics and vibration*. Boca Raton, Florida: CRC Press, 2015.

[12] R. Panneton and N. Atalla, "Numerical prediction of sound transmission through finite multilayer systems with poroelastic materials," *The Journal of the Acoustical Society of America*, vol. 100, pp. 346–354, 7 1996.

[13] J. Allard and N. Atalla, *Propagation of Sound in Porous Media: Modelling Sound Absorbing Materials*. Wiley-Blackwell, 2 ed., 2009.

[14] T. Vigran, *Building Acoustics*. CRC Press, 2 ed., 2019.

[15] Y. Yu and C. Hopkins, "Reduced order integration for the radiation efficiency of a rectangular plate," *JASA Express Letters*, vol. 1, p. 062801, 6 2021.

[16] M. E. Terzakis, C. Van hoorickx, and M. Hornikx, "Spatial windowing for finite-size incident sound transmission coefficient of multi-component surfaces," *INTER-NOISE and NOISE-CON Congress and Conference Proceedings*, vol. 270, pp. 2900–2909, 10 2024.

[17] T. Vigran, "Predicting the sound reduction index of finite size specimen by a simplified spatial windowing technique," *Journal of Sound and Vibration*, vol. 325, pp. 507–512, 8 2009.

[18] T. Vigran, "Sound transmission in multilayered structures – Introducing finite structural connections in the transfer matrix method," *Applied Acoustics*, vol. 71, pp. 39–44, 1 2010.

[19] A. Santoni, P. Bonfiglio, P. Fausti, and N. Z. Martello, "Sound insulation of heavyweight walls with linings and additional layers: numerical investigation," in *EuroNoise 2015*, (Maastricht), pp. 2537–2542, 2015.

[20] J. Proakis and D. Manolakis, "Design of Digital Filters," in *Digital Signal Processing*, ch. 10, pp. 660–664, Pearson, 4 ed., 2006.

[21] M. E. Terzakis, C. Van hoorickx, and M. Hornikx, "Characterization of façade sound insulation by impulse response measurements for various source position formats: a case study," *INTER-NOISE and NOISE-CON Congress and Conference Proceedings*, vol. 270, pp. 2910–2920, 10 2024.

[22] ISO, "ISO 3382-2:2008 Acoustic - Measurement of Room Acoustic Parameters, Part 2: Reverberation Time in Ordinary Rooms," *International Organization for Standardization*, 2008.

[23] G. James, D. Witten, T. Hastie, and R. Tibshirani, *An Introduction to Statistical Learning with Applications in R*. New York, NY: Springer US, 2021.

[24] M. N. Wright and A. Ziegler, "ranger : A Fast Implementation of Random Forests for High Dimensional Data in C++ and R," *Journal of Statistical Software*, vol. 77, no. 1, 2017.

[25] G. James, D. Witten, T. Hastie, and R. Tibshirani, "Resampling Methods," in *An Introduction to Statistical Learning*, pp. 203–205, Springer US, 2021.

[26] E. Bartz and T. Beielstein, *Hyperparameter tuning and optimization applications. In: Hyperparameter tuning for machine and deep learning with R: a practical guide.* Springer, 2023.

[27] E. Murphy and E. A. King, "Principles of Environmental Noise," in *Environmental Noise Pollution*, pp. 9–49, Elsevier, 2014.